Scientific Research Publishing

Smart Grid and Renewable Energy, 2023, 14, 197-208
https://www.scirp.org/journal/sgre
ISSN Online: 2151-4844
ISSN Print: 2151-481X

Establishment of a Model for the Calculation of the COP of a Solar Adsorption Refrigerator

Amadou Konfe, Gilbert G. Nana, Salif Ouedraogo, Sié Kam

Laboratory of Thermal and Renewable Energies, University Joseph Ki-Zerbo, Ouagadougou, Burkina Faso
Email: konfeamadou@gmail.com

How to cite this paper: Konfe, A., Nana, G.G., Ouedraogo, S. and Kam, S. (2023) Establishment of a Model for the Calculation of the COP of a Solar Adsorption Refrigerator. *Smart Grid and Renewable Energy*, **14**, 197-208.
https://doi.org/10.4236/sgre.2023.1411012

Received: October 5, 2023
Accepted: November 26, 2023
Published: November 29, 2023

Abstract

This paper deals with the evaluation of the Coefficient of Performance (COP) of solar adsorption refrigeration. In the literature, simulation models to predict the thermal behaviour and the coefficient of performance of these systems are uncommon. This is why we suggest a model to simulate the operation of the machine in a typical hot and dry climate of the city of Ouagadougou. The objective is to provide a model for calculating the COP from the measurement of the ambient temperature and the irradiation of a given site. Starting from mathematical modelling, a resolution and simulation were made with COMSOL software based on the Dubinin-Astakhov adsorption model, the heat transfer balance equations, and the Linear Driving Force (LDF) model to describe the thermal behaviour of the system. A one-week measurement sequence on the adsorption solar refrigerator at the Albert Schweitzer Ecological Centre (CEAS) validated the numerical results. The measurement shows that for the days with high sunshine, the temperature of the reaction medium reaches 110˚C, and the pressure reaches 500 mbar. This leads to a production of cold that allows it to reach the temperature of −5˚C at the evaporator. Under these conditions, the COP is worth 14%. These results are obtained both by numerical simulation using the COMSOL 5.1 software and after a measurement session on the solar refrigerator available to the CEAS. We obtained an experimental and theoretical coefficient of performance varying between 9% and 14% with a difference of between 0% and 3%. We conclude that our model is suitable to estimate the COP of any device based on its thermal properties, the ambient temperature and the irradiation of a given site.

Keywords

Solar, Refrigeration, Adsorption, Coefficient of Performance, Modelling

1. Introduction

Solar refrigeration is an important application of solar thermal due to the excellent agreement between the duration of sunshine and energy needs [1] [2]. In developing countries, this type of system can be an interesting way to produce cold from solar energy. Indeed, Burkina Faso, like other countries with a dry tropical climate has a very significant solar potential whose average is estimated at 5.5 kWh/m^2/day [2]. In addition, out-of-town areas are often not connected to the electricity grid. The use of solar adsorption refrigerators thus improves the living conditions in these areas from a health and economic point of view. Several small prototypes, experimented with different adsorption pairs both in the laboratory and *in situ* in different climates [3] [4] [5], have demonstrated the feasibility of the process.

Research for optimal operating conditions is necessary. For this purpose, one of the essential questions is the determination of the parameters to obtain a high COP.

Simulation models to predict the thermal behaviour and the coefficient of performance of these systems are uncommon.

This is why we suggest a model to simulate the operation of the machine in a typical hot and dry climate of the city of Ouagadougou.

2. System Modelling

The solar reactor which is the subject of our investigations is the driving element that plays the role of compressor in the above-mentioned adsorption refrigerating machine. This unit, shown in **Figure 1**, works with the activated carbon/methanol pair for ice production to store vaccines and other pharmaceuticals. The reactor is alternately connected to a condenser and an evaporator by valves. This is a box containing a diffuser which consists of a grid arranged in the form of a triangle. A triangle in two is filled with adsorbent, while the others remain free to allow the passage of the adsorbate to the condenser.

2.1. Simplify Hypotheses

1) The three phases (solid, adsorbed and gaseous) of the adsorbate are considered to be at each point in thermodynamic equilibrium. This makes it possible to define only a single equivalent temperature for these three phases and to replace the reactive medium with an equivalent continuous medium, thus characterized by an equivalent thermal conductivity.

2) Given the low flow rate of the desorbed refrigerant, the convective heat transfer in the vapor phase is neglected.

3) The pressure losses are negligible in the adsorbent bed, so at each instant, the pressure of the adsorbate is uniform in the reactor, but it can however vary over time.

4) Resistance to mass transfer in micropores and macropores and in interstitial spaces is negligible.

Figure 1. Picture of the CEAS device.

5) Except for the adsorbate, the physical properties of the adsorbent and the metal walls of the adsorber are considered constant.

6) The losses of the side walls of the solar reactor are negligible.

2.2. Balance Equations

The different heat exchanges at the reactor are shown schematically in **Figure 2**.

The heat balance on the radiation window is given by:

$$\left(m\cdot C_p\right)_v \frac{\mathrm{d}T_v}{\mathrm{d}t} = a_g IS + S\left(h_r + h_c\right)\left(T - T_v\right) + S\left(h_{ra} + h_{ca}\right)\left(T_{amb} - T_v\right) \quad (1)$$

where h_r and h_c are respectively the heat transfer coefficients by radiation and by conduction between the glass and the metal parts of the adsorber. h_{ra} and h_{ca} are respectively the heat transfer coefficients by radiation and by conduction between the window and the environment; T_{amb} is the ambient temperature and that of the reaction medium; I is the solar radiation per unit time and per unit area, S is the sensor area and a_g the absorption coefficient of the glass.

Energy and mass balance of the reaction medium:

$$\left(m_a Cp_a + m\cdot m_a Cp_l + m_g Cp_g\right)\frac{\partial T}{\partial t} = IS\eta_c + \left(h_r + h_c\right)S\left(T_v - T\right) + Q\left(t\right) \quad (2)$$

where $Q(t)$ represents the temporal term heat source from the heat of adsorption (or desorption); Cp_a represents the specific heat of the adsorbent; Cp_l represents the specific heat of the adsorbate; Cp_g represents the specific heat of the metallic material; m_a is the mass of the adsorbent; m_g is the mass of the metallic material.

The mass transfer equation is obtained taking into account Assumptions 3 and 4:

$$m_a \frac{\partial m}{\partial t} = Q' \quad (3)$$

where Q' represents the term source of adsorption mass (or desorption) and is related with isosteric heat of adsorption by the following equation:

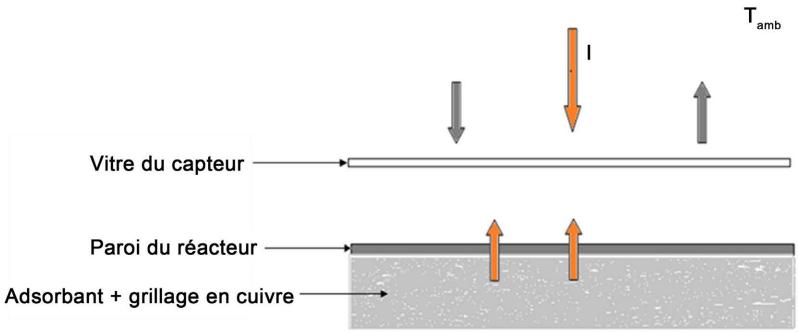

Figure 2. Exchange balance at the solar reactor.

$$Q = Q_{isost} Q' = Q_{isost} m_a \frac{\partial m}{\partial t} \tag{4}$$

So, the general energy conservation equation combined with the mass conservation equation becomes:

$$\left(m_a Cp_a + m \cdot m_a Cp_l + m_g Cp_g\right)\frac{\partial T}{\partial t} = IS\eta_c + \left(h_r + h_c\right)S\left(T_v - T\right) + Q_{isost} m_a \frac{\partial m}{\partial t} \tag{5}$$

where η_c represents the efficiency of the solar collector. It should be noted that:

- During the desorption phase:

$$Q(t) = +Q_{isost} m_a \frac{\partial m}{\partial t} \tag{61}$$

$$\text{where} \quad Q_{isost} > 0 \quad \text{et} \quad \frac{\partial m}{\partial t} < 0 \tag{72}$$

Which means that during this phase of desorption $Q(t)$ represents a term of well.

- During the adsorption phase:

$$Q(t) = -Q_{isost} m_a \frac{\partial m}{\partial t} \tag{8}3$$

$$\text{where,} \quad Q_{isost} < 0 \quad \text{et} \quad \frac{\partial m}{\partial t} > 0 \tag{9}$$

So, during adsorption, $Q(t)$ represents a source term.

We use the Dubinin-Astakhov model for calculating adsorbed mass as a function of temperature and pressure. We recall here the main equation of this model:

$$m = w_0 \rho(T) \exp\left[-D\left(T \ln \frac{P_s(T)}{P}\right)^n\right] \tag{10}$$

The differentiation of Equation (10) leads to:

$$\frac{\partial m}{\partial t} = nDmT^n \left(\ln \frac{P_s(T)}{P}\right)^{n-1} \left[\frac{\mathrm{d} \ln P}{\mathrm{d}t} - \frac{Q_{isost}}{RT^2} \frac{\mathrm{d}T}{\mathrm{d}t}\right] \tag{11}$$

Substituting Equations (10) and (11) in Equation (5), we obtain the final equation of heat and mass transfer in the reactive medium:

$$\left(m_a Cp_a + m \cdot m_a Cp_l + m_g Cp_g + \frac{bQ_{isost}^2}{RT^2}\right)\frac{\partial T}{\partial t} = IS(h_c) + (h_r + h_c)S(T_v - T) + Q_{isost} b \frac{\mathrm{d}\ln P}{\mathrm{d}t} \quad (12)$$

$$\text{With,} \quad b = m_a nDmT^n \left(\ln \frac{P_s(T)}{P}\right)^{n-1} \quad (13)$$

Initial conditions

At initial time, we assume a uniform distribution of temperature throughout the reactor equal to the ambient temperature at sunrise. The pressure is assumed equal to the evaporation pressure and corresponds to the saturation pressure at the evaporation temperature. Therefore, the initial adsorbed mass is equal to $m(T_{amb}, P_e)$.

$$T(t=0) = T_{amb} \quad (14)$$

$$P(t=0) = P_e = P_s(T_e) \quad (15)$$

$$m = m(T_{amb}, P_e) \quad (16)$$

$$T_v(t=0) = T_{amb} \quad (17)$$

2.3. Determination of Transfer Coefficients

The transfer coefficients are given by Melkon Tatlıer and Ayşe Erdem-Şenatalar [6].

$$h_r = \frac{\sigma(T_v + T)(T_v^2 + T^2)}{(1/\varepsilon_v) + (1/\varepsilon_g)} \quad (18)$$

$$h_c = 1.65 + 0.025(T - T_v) \quad (19)$$

$$h_{ra} = \varepsilon_v \sigma (T_v + T_{amb})(T_v^2 + T_{amb}^2) \quad (204)$$

$$h_{ca} = 5.7 + 3.8V \quad (21)$$

where V is the wind speed; σ the Stefan-Boltzmann constant; ε_v and ε_g are respectively the emissivity of the glass and the emissivity of the metal walls of the adsorber.

2.4. Pressure Conditions

Recall that during the isosteric phases (cooling heating), the reactor is isolated on itself, the variation of the total mass of adsorbed water is zero. This condition is expressed by:

$$\frac{\partial m}{\partial t} = 0 \quad (22)$$

So the general equation during these two phases is written:

$$\left(m_a Cp_a + m \cdot m_a Cp_l + m_g Cp_g\right)\frac{\partial T}{\partial t} = IS(\eta_c) + (h_r + h_c)S(T_v - T) \quad (23)$$

On the other hand, during the period of desorption-condensation or evapora-

tion-adsorption, the pressure is imposed by the pressure of the condenser or the pressure of the evaporator, respectively. This simplifies the general equation of heat and mass transfer during the two isobaric phases to the following equation:

$$\left(m_a Cp_a + m \cdot m_a Cp_l + m_g Cp_g + \frac{bQ_{isost}^2}{RT^2}\right)\frac{\partial T}{\partial t} = IS\left(\eta_c\right) + \left(h_r + h_c\right)S\left(T_v - T\right) \quad (245)$$

2.5. First-Order Internal Kinetics Model (LDF)

Since the kinetics of adsorption and desorption are no longer instantaneous but dependent on the mass gradient existing between the current mass of the adsorbed phase and that at equilibrium, the equation governing the kinetics is written:

$$\frac{\partial m}{\partial t} = K\left(m_e - m(t)\right) \quad (25)$$

Since the gradient is assumed to be linear, this model is called LDF (Linear Driving Force).

This model is widely used by different authors [7]-[13].

The constant K of Equation (25) represents the effective mass transfer coefficient inside the pores. The definition of this coefficient requires knowledge of the different conditions that limit the kinetics (high-pressure molecular diffusion, Knudsen diffusion at low pressure [11]).

In general, a simplified approach is used, it consists of taking for K value:

$$K = \frac{15D_e}{R_p^2} \quad (26)$$

where R_p is the adsorbent particle radius.

D_e is the effective diffusivity, which varies with temperature according to the Arrhenius equation [12]:

$$D_e = D_0 \exp\left(\frac{-E_a}{RT}\right) \quad (27)$$

where,

E_a represents the activation energy of the diffusion process. D_0 is a pre-exponential factor.

Finally, Equation (1) is written as:

$$\frac{\mathrm{d}m}{\mathrm{d}t} = \frac{15D_0}{r^2}\exp\left(\frac{-E_a}{RT}\right)\left(m_e - m\right) \quad (28)$$

2.6. Solar Performance Coefficient COP_s

The solar performance coefficient of a solar COP_s refrigerating machine is defined as the ratio between the amount of cold produced at the evaporator and the total solar energy incident during a full day [1] [13]:

$$COP_s = \frac{Q_f}{I_t * S} \quad (29)$$

With,

$$Q_f = ma\left(\Delta mL - \int_{Tc}^{Te} Cp\right) \tag{306}$$

$$I_t = \int_{\text{lever du soleil}}^{\text{coucher du soleil}} I(t)\,\mathrm{d}t \tag{317}$$

where S is the surface of the sensor; $I(t)$ is the instantaneous solar radiation.

3. Experimental Device

For the measurement sessions, we have:

- Type K thermocouples placed in such a way as to obtain the temperature of the outer surface of the generator tube, the condenser, the cold room and the instantaneous irradiation. These values are given with an accuracy of 1%;
- A mechanical manometer that tracks the evolution of the generator pressure;
- A LOGGER GL200A and GRAPHTEC Midi data logger which allows data logging. This experimental device is summarized in **Figure 3**.

4. Resolution Method

The method of solving the system of Equations (1) to (30) was performed using the PDE of the COMSOL 5.1 numerical simulation software to describe the transient behavior of the solar reactor. The parameters used in this simulation are:

Copper is used as mass adsorber building materials $m_g = 5\,\text{kg}$ and the specific heat of the adsorber is $Cp_g = 0.380\,\text{kJ/kg}\cdot\text{K}$.

Dubbininasthakov parameters and physical constants for the activated carbon/methanol pair (Pons *et al.*) [14] [15]:

Maximum activated carbon adsorption capacity 35: W_0(l/kg) = 0.425.

Constant of Dubinin Astakhov: D = 5.02e−7; n = 2.15.

Specific heat of the adsorbent: $Cp_a = 0.920\,\text{kJ/kg}\cdot\text{K}$.

Mass of the adsorbent: $m_a = 1\,\text{kg}$.

5. Results and Discussion

We present in this part the different results obtained from the model resolution developed above.

Figure 4 shows the distribution of temperature, pressure and sunshine in the reactor as a function of time over a measurement sequence from 23 to 26 April 2023.

The curves in **Figure 4** represent the evolution of the temperature within the adsorber, the condenser and the evaporator during the period from April 23 to April 26, 2023. The maximum sunshine recorded remains greater than 1000 W/m^2. These values correspond to temperatures of the adsorber sometimes reaching 110˚C. This value is lower than the decomposition threshold temperature of methanol which is of the order of. There is therefore no risk of malfunction

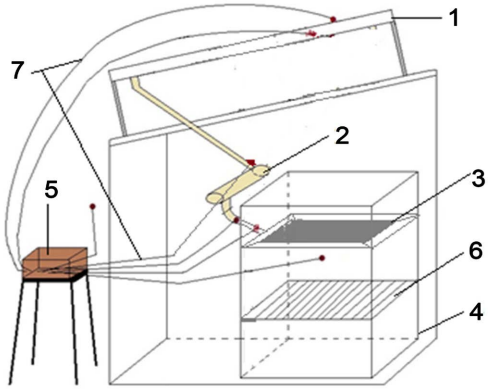

1: sensor; 2: condenser; 3: evaporator; 4: sideboard;
5: datalogger; 6: rack; 7: thermocouples.

Figure 3. Diagram of the experimental device.

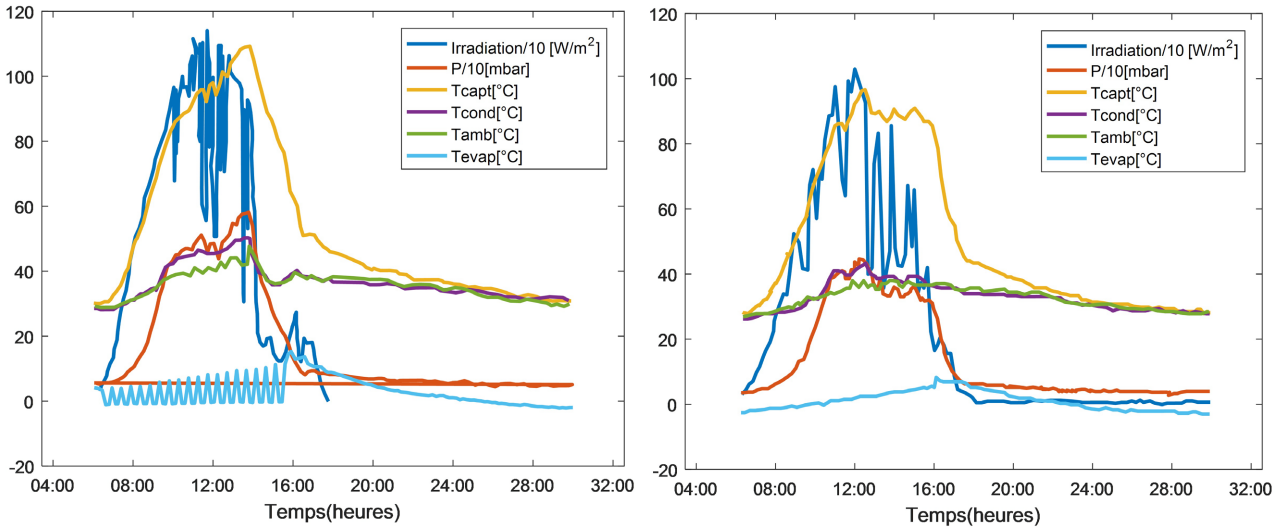

(a) 23/04/2023

(b) 24/04/2023

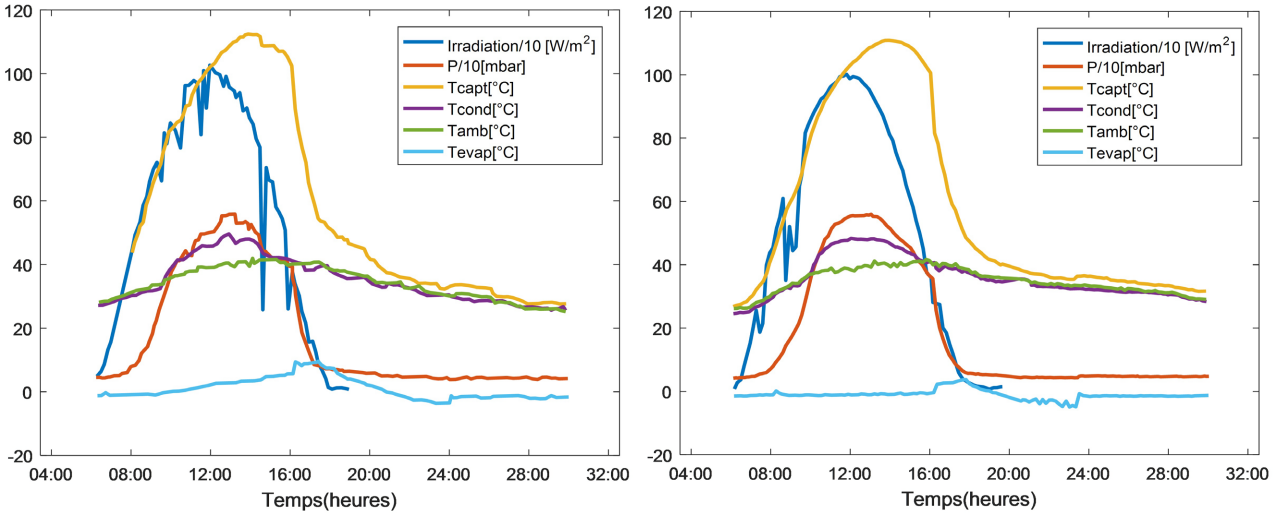

(c) 25/04/2023

(d) 26/04/2023

Figure 4. Distribution of temperatures, pressure and sunshine in the system.

of the cold production cycle. In addition, the temperature of the condenser is almost equal to the ambient temperature during a cycle of operation, except for the time interval between 08 hours and 16 hours when the difference sometimes reaches 14˚C. This moment corresponds to the desorption of methanol that arrives in the condenser with a temperature close to that of the adsorbent bed, hence this difference. This difference may also depend on the amount of gas desorbed and the weather conditions of the day. In addition, the temperature evolution curves recorded at the evaporator show that there is cold production during a 24-hour cycle because the minimum temperature is reached −5˚C. The amount of cold drawn off is all the more important than the amount of desorbed methanol is high, and therefore a good sunning of the sensor. On these curves, there is a temperature jump of around 16 hours and then a sudden fall. This rise in temperature can be explained by the contribution of the sensible heat of the sensor because, during this period of the cycle, the latter is put into communication with the evaporator.

Figure 4 also shows the variation curves of the pressure within the adsorbate bed. It can be seen that the pressure evolves with irradiation and that the ranges of values are almost identical and below atmospheric pressure. These beaches are between 50 mbar and 500 mbar. The maximum values are reached for the best irradiated days. Note that when the pressure of the reaction medium is high, the amount of desorbed methanol is large and there is an increase in the production of cold.

For it to have desorption, it must be adsorption. In what follows, we present the curves of variation of the mass of methanol adsorbed during the measurement period and those obtained by numerical simulation as shown in Figure 5.

We note that the theoretical and experimental curves have the same paces. These curves show that the quantity of refrigerant adsorbed by the activated carbon varies during a 24-hour cycle. This quantity decreases between 08 hours and 16 hours which corresponds to the desorption—condensation phase but increases at the end of the day until the beginning of a new cycle. This is explained by the fact that in this period, it adsorption and production of cold. It is also observed that the desorption is not total (minimum value greater than zero). This can be explained on the one hand by the properties of activated carbon and on the other hand by the level of heating of the reaction medium. The days of good sunshine lead to better desorption of methanol. In order to better appreciate the results mentioned above, we summarize in Table 1 the values of the system performance coefficient obtained during a measurement sequence of one week. These values are calculated from Equation (29).

Table 1 shows that the experimental and theoretical COP varies between 9% and 14%.

So, there is a good agreement. The same similarity is observed in the amount of cold drawn off at the evaporator. For experimental results, the maximum COP is obtained during the day of April 23, 2023.

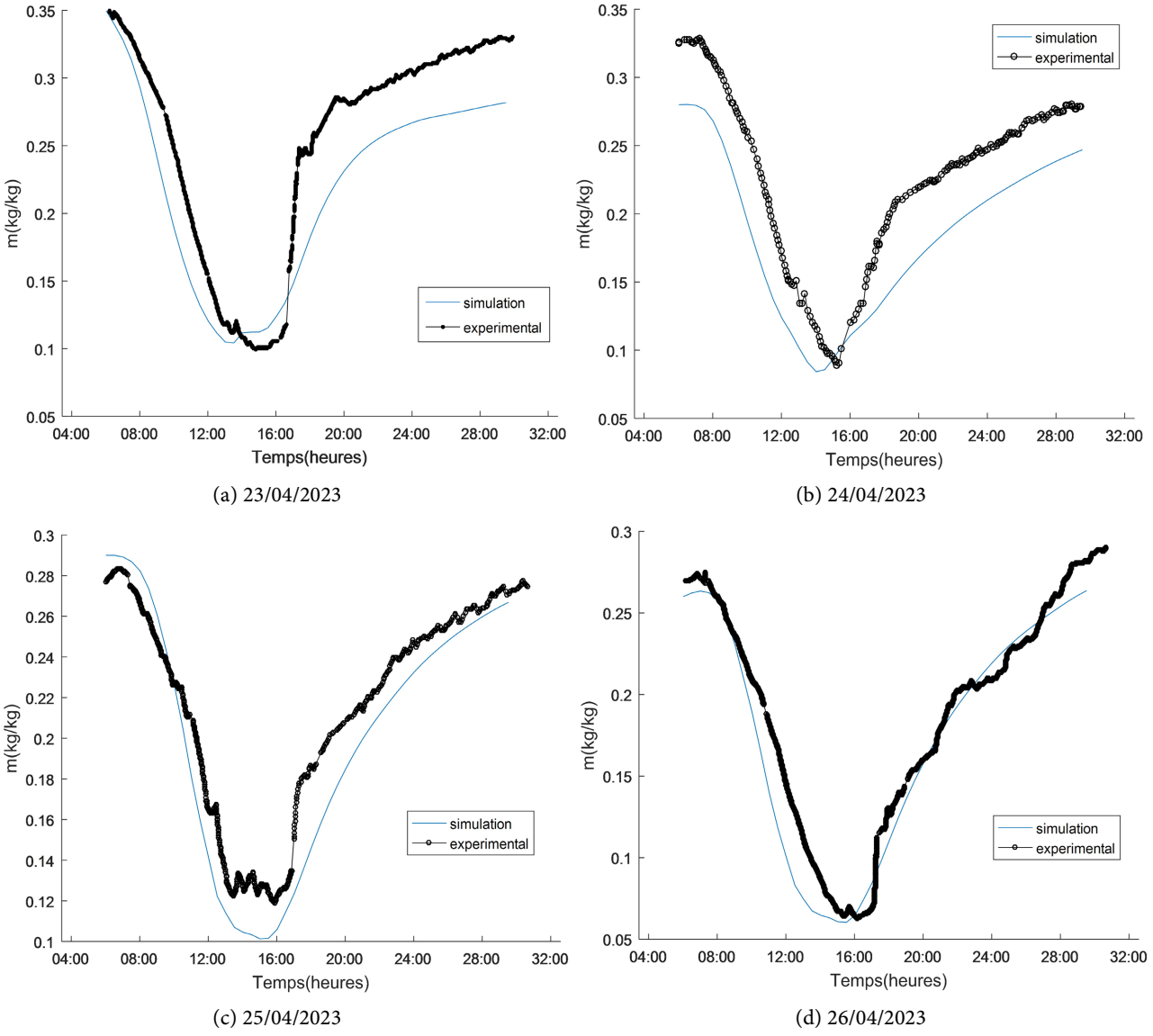

(a) 23/04/2023

(b) 24/04/2023

(c) 25/04/2023

(d) 26/04/2023

Figure 5. Adsorbed mass profile from 23 to 26 April 2015.

Table 1. Theoretical and experimental results.

	Amount of cold (MJ)		Coefficient of Performance (COP) solar		Difference (%)
Date	Measured	Simulated	Measured	Simulated	
22-04-2023	3.03	3.32	13	14	1
23-05-2023	2.90	2.37	14	11	3
24-05-2023	1.99	2.28	10	12	2
25-05-2023	2.75	2.36	11	9	2
26-05-2023	2.70	2.37	11	10	1
27-05-2023	2.47	2.41	12	12	0
28-05-2023	1.81	2.50	9	12	3

Given the good agreement between the experimental and simulation results, we can validate our model.

6. Conclusions

At the end of this study, we studied the influence of ambient temperature and sunshine on the temperature of the collector, the condenser, the evaporator, the mass of cycled methanol and the pressure of the reaction medium. For example, for good days of sunshine, the temperature of the reaction medium reaches 110˚C, and the pressure reaches 500 mbar. This leads to a production of cold that allows it to reach the temperature of −5˚C at the evaporator.

We obtained an experimental and theoretical coefficient of performance varying between 9% and 14% with a difference of between 0% and 3%.

We conclude that our model is suitable to estimate the COP of any device based on its thermal properties, the ambient temperature and the irradiation of a given site.

Even if simplifying hypotheses have produced results in line with experimental ones, it is necessary to take them into account in order to see their influence.

Also, our model needs to be applied to several devices to confirm its validation.

Acknowledgements

The ISP, Uppsala University, Sweden is gratefully acknowledged for their support of project BUF01.

Conflicts of Interest

The authors declare no conflicts of interest regarding the publication of this paper.

References

[1] Wassila, C. (2008) Etude et Analyse d'une machine frigorifique solaire à adsorption. Ph.D. Thesis, Université Mentouri Constantine, Constantine.

[2] Konfe, A. (2017) Étude Thermique et Conception d'un Réfrigérateur Solaire à Adsorption. Ph.D. Thesis, Université Ouaga I Pr Joseph Ki-Zerbo, Ouagadougou.

[3] Rezk, A.R.M. (2012) Theoretical and Experimental Investigation of Silica Gel/Water Adsorption Refrigeration Systems. Ph.D. Thesis, University of Birmingham, Birmingham. http://etheses.bham.ac.uk/3623/

[4] Wang, D.C., Zhang, J.P., Tian, X.L., Liu, D.W. and Sumathy, K. (2014) Progress in Silica Gel-Water Adsorption Refrigeration Technology. *Renewable and Sustainable Energy Reviews*, **30**, 85-104. https://doi.org/10.1016/j.rser.2013.09.023

[5] Alahmer, A. and Ajib, S. (2020) Solar Cooling Technologies: State of Art and Perspectives. *Energy Conversion and Management*, **214**, Article ID: 112896. https://doi.org/10.1016/j.enconman.2020.112896

[6] Tatlıer, M. and Erdem-Şenatalar, A. (1999) The Effects of Thermal Gradients in a Solar Adsorption Heat Pump Utilizing the Zeolite-Water Pair. *Applied Thermal Engineering*, **19**, 1157-1172. https://doi.org/10.1016/S1359-4311(98)00113-6

[7] Dubinin, M.M. and Astakhov, V.A. (1971) Description of Adsorption Equilibria of

Vapors on Zeolithe over Wide Ranges of Temperature and Pressure. In: Flanigen, E., et al., Eds., *Molecular Sieve Zeolites-II*, Vol. 102, Advances in Chemistry, American Chemical Society, Washington DC, 69-85.
https://doi.org/10.1021/ba-1971-0102.ch044

[8] Suzukl, M. (1990) Adsorption Engineering. Kodansha, Tokyo.

[9] Cacciola, G. and Restuccia, G. (1995) Reversible Adsorption Heat Pump: A Thermodynamic Model. *International Journal of Refrigeration*, **18**, 100-106.
https://doi.org/10.1016/0140-7007(94)00005-I

[10] Mimet, A. (1991) Etude théorique et expérimentale d'une machine frigorifique à adsorption d'ammoniac sur charbon actif. FPMS Mons, Mons.

[11] Hildbrand, C., Dind, P., Pons, M. and Buchter, F. (2004) A New Solar Powered Adsorption Refrigerator with High Performance. *Solar Energy*, **77**, 311-318.
https://doi.org/10.1016/j.solener.2004.05.007

[12] Faghri, A. and Zhang, Y.W. (2006) Transport Phenomena in Multiphase Systems. Academic Press, Cambridge. https://doi.org/10.1016/B978-0-12-370610-2.50007-6

[13] Guilleminot, J.J. and Meunier, F. (1981) Eude expérimentale d'une glacière solaire utilisant le cycle zéolithe-eau. *Revue Générale de Thermique*, **239**, Article ID: 825834.

[14] Pons, M., *et al.* (2012) Performance Comparison of Six Solar-Powered Air-Conditioners Operated in Five Places. *Energy*, **46**, 471-483.
https://doi.org/10.1016/j.energy.2012.08.002

[15] Pons, M. and Grenier, Ph. (1986) A Phenomenological Adsorption Equilibrium Law Extracted from Experimental and Theoretical Considerations Applied to the Activated Carbon + Methanol Pair. *Carbon*, **24**, 615-625.
https://doi.org/10.1016/0008-6223(86)90151-X